

Coordination Chemistry Fundamentals

Instrumental Analysis of Coordination Compounds

Volume 2

Edited by Hiroki Oshio and Graham N. Newton



Instrumental Analysis of Coordination Compounds
Volume 2

Coordination Chemistry Fundamentals Series

Series editors:

Shigehisa Akine, *Kanazawa University, Japan*
Yasuhiro Funahashi, *Osaka University, Japan*
Osamu Ishitani, *Tokyo Institute of Technology, Japan*
Hiroshi Nakazawa, *Osaka Metropolitan University, Japan*
Hidetaka Nakai, *Kindai University, Japan*
Yasuhiro Ohki, *Kyoto University, Japan*
Toshio Yamaguchi, *Fukuoka University, Japan/Qinghai Institute of Salt Lakes, CAS, China*

Titles in the series:

- 1: Organometallic Chemistry
- 2: Metal Ions and Complexes in Solution
- 3: Coordination Chemistry: Molecular Science of Organic–Inorganic Complexes
- 4: Instrumental Analysis of Coordination Compounds: Volume 1
- 5: Instrumental Analysis of Coordination Compounds: Volume 2

How to obtain future titles on publication:

A standing order plan is available for this series. A standing order will bring delivery of each new volume immediately on publication.

For further information please contact:

Book Sales Department, Royal Society of Chemistry, Thomas Graham House, Science Park, Milton Road, Cambridge, CB4 0WF, UK
Telephone: +44 (0)1223 420066, Fax: +44 (0)1223 420247
Email: booksales@rsc.org
Visit our website at books.rsc.org

Instrumental Analysis of Coordination Compounds

Volume 2

Edited by

Hiroki Oshio

Dalian University of Technology

Email: oshio@chem.tsukuba.ac.jp

and

Graham N. Newton

University of Nottingham, UK

Email: Graham.Newton@nottingham.ac.uk



Coordination Chemistry Fundamentals Series No. 5

Print ISBN: 978-1-83767-481-7

Two-volume set print ISBN: 978-1-83767-373-5

PDF ISBN: 978-1-83767-499-2

EPUB ISBN: 978-1-83767-500-5

Print ISSN: 2635-1498

Electronic ISSN: 2635-1501

A catalogue record for this book is available from the British Library

© Japan Society of Coordination Chemistry 2024

All rights reserved

Translation from the Japanese language edition:

Sakutai Kagaku Sensho 7 – Kinzokusakutai No Kikibunnseki (Gekan),
edited by Hiroki Oshio

ISBN: 978-4-7827-0640-4

Copyright © 2012 Japan Society of Coordination Chemistry

All Rights Reserved

Apart from fair dealing for the purposes of research for non-commercial purposes or for private study, criticism or review, as permitted under the Copyright, Designs and Patents Act 1988 and the Copyright and Related Rights Regulations 2003, this publication may not be reproduced, stored or transmitted, in any form or by any means, without the prior permission in writing of The Royal Society of Chemistry or the copyright owner, or in the case of reproduction in accordance with the terms of licences issued by the Copyright Licensing Agency in the UK, or in accordance with the terms of the licences issued by the appropriate Reproduction Rights Organization outside the UK. Enquiries concerning reproduction outside the terms stated here should be sent to The Royal Society of Chemistry at the address printed on this page.

Whilst this material has been produced with all due care, The Royal Society of Chemistry cannot be held responsible or liable for its accuracy and completeness, nor for any consequences arising from any errors or the use of the information contained in this publication. The publication of advertisements does not constitute any endorsement by The Royal Society of Chemistry or Authors of any products advertised. The views and opinions advanced by contributors do not necessarily reflect those of The Royal Society of Chemistry which shall not be liable for any resulting loss or damage arising as a result of reliance upon this material.

The Royal Society of Chemistry is a charity, registered in England and Wales, Number 207890, and a company incorporated in England by Royal Charter (Registered No. RC000524), registered office: Burlington House, Piccadilly, London W1J 0BA, UK, Telephone: +44 (0)20 7437 8656.

For further information see our website at www.rsc.org

Printed in the United Kingdom by CPI Group (UK) Ltd, Croydon, CR0 4YY, UK.

Preface

The 1950s are often referred to as the Renaissance of inorganic compounds, yet the true significance of metal complexes was only fully realized in the latter half of the 20th century. Research in metal complexes spans a broad spectrum of topics, from syntheses and reactions to structures and physical properties. The instrumental analysis of metal complexes is critical to the field, and can often lead to the thrilling discovery of unexpected phenomena. The breadth of measurement and analysis techniques that are now available dictate that the coordination chemist should have wide-ranging knowledge of areas such as quantum chemistry, thermodynamics, kinetics, equilibrium theory, analytical chemistry, surface chemistry, and solid-state chemistry, to name but a few. This book not only explains the methods but also the principles of the measurements and the fundamental theory required to ensure that data can be collected and interpreted correctly and the necessary information can be extracted.

We could not measure physical properties in our labs or institutes a half-century ago. First, we booked the instruments and waited for days or weeks for the measurements. Some measurements themselves took several days, but we did not feel it was inconvenient. The data obtained through a combination of time and effort were valuable, and the results made us happy or sometimes disappointed. Nowadays, however, labs and institutes are filled with analytical instruments, from everyday workhorse tools used in every undergraduate lab to advanced developmental pieces of equipment that are rarely used.

Instruments have generally been improved from analog to digital, and anyone can easily obtain data by pressing the START button. However, the more convenient it becomes, the more we are accustomed to always having the data and the less impressed we are. Last century, in a more inconvenient era, we had the time to learn about the measurements while waiting for

access or data collection to complete. Since measurement data were rarely obtained, we could ponder the obtained spectrum and the sequence of numbers all night long. It is generally believed that “more convenience enriches society,” and so the world of instrumental analysis has developed steadily. However, we may sometimes feel, “There is no need to make everything more convenient.” We need more time to face the measurements and consider the obtained data.

This book serves as a comprehensive commentary and introduction to instrumental analyses of metal complexes, a valuable resource for all chemists. It covers nearly all the instruments necessary for modern research, meeting the demands of this era. However, it's essential for the reader not to be complacent with this book alone. They should be inspired to strive for a deeper understanding by exploring the more specialized books referenced in this text, fostering a continuous learning mindset.

A deeper understanding will foster intuition and lead to discovery.

Hiroki Oshio and Graham N. Newton

Contents

Instrumental Analysis of Coordination Compounds – Volume 1

Chapter 1	Ligand Field Theory	1
<i>Sumio Kaizaki</i>		
1.1	Introduction	1
1.2	Crystal Field Theory	1
1.2.1	Orbital Energy	1
1.2.2	Crystal Field Splitting	2
1.2.3	Weak Field and Strong Field	4
1.2.4	Ligand Field Theory and the Tanabe–Sugano Diagram	10
1.2.5	Ligand Field Parameters for Low Symmetry Field	12
1.3	Angular Overlap Model	14
1.3.1	Additivity, Holohedrized Symmetry and Transferability	18
Appendix A		22
Further Reading		26
References		26
Chapter 2	Optical Spectroscopy	27
<i>Sumio Kaizaki</i>		
2.1	Introduction	27
2.1.1	Electronic Spectra	28
2.1.2	Chiroptical Spectra	51

Further Reading	61
References	63
Chapter 3 Acid Dissociation Constants, Formation Constants, and Other Thermodynamic Parameters	65
<i>Ryo Kanzaki</i>	
3.1 Equilibrium in Solutions	66
3.1.1 Stability Constants	66
3.1.2 Law of Conservation of Mass (Mass Balance Equation)	67
3.1.3 Acid Dissociation Constants of Ligands	68
3.1.4 Calculation of Formation Distribution from Stability Constants	70
3.1.5 Solvates	72
3.2 Determination of Stability Constants and Other Thermodynamic Parameters	73
3.2.1 Potentiometry	73
3.2.2 Stability Constant Determination by pH Titration	75
3.2.3 Spectrometry	76
3.2.4 Calorimetry	80
3.2.5 Rate Constants	83
3.3 Complexation Thermodynamics	86
3.3.1 Gibbs Energy and Stability Constants	86
3.3.2 Supporting Electrolytes and Ionic Strength	87
3.3.3 Enthalpy and Entropy	88
3.3.4 Reaction Rates and Activation State	89
References	91
Chapter 4 Electrochemistry	92
<i>Ryota Sakamoto and Hiroshi Nishihara</i>	
4.1 Nernst Equation	92
4.2 Electrolyte Solution	93
4.2.1 Solvent	93
4.2.2 Supporting Electrolyte	94
4.3 Electrode	94
4.3.1 Working Electrode	94
4.3.2 Reference Electrode	95
4.3.3 Counter Electrode	97
4.3.4 Arrangement of Electrodes	98

4.4	Electric Double Layer	100
4.5	Potential Window	100
4.6	Apparatus	102
4.7	Charge Transfer and Diffusion Limitation	102
4.7.1	Charge Transfer Limitation	102
4.7.2	Diffusion Limitation	104
4.7.3	Current–Potential Curve Taking Mass Transfer Into Account	106
4.7.4	Reversible, Quasi-reversible, and Irreversible Systems	107
4.8	Measurement Techniques	108
4.8.1	Chronoamperometry	108
4.8.2	Chronocoulometry	109
4.8.3	Measurements with a Rotating Disk Electrode	109
4.8.4	Tafel Plot	110
4.8.5	Pulse Voltammetry	111
4.8.6	Cyclic Voltammetry	113
4.8.7	Bulk Electrolysis	116
4.8.8	UV-visible–NIR Spectroscopy Upon Electrolysis	118
4.8.9	Surface Modified Electrode	119
	References	119
Chapter 5	Calorimetry and Thermal Analysis	121
	<i>Kazuya Saito</i>	
5.1	Thermal Analysis	121
5.1.1	Introduction	121
5.1.2	Differential Thermal Analysis and Differential Scanning Calorimetry	123
5.1.3	Thermogravimetry	136
5.2	Heat Capacity Calorimetry	140
5.2.1	Thermodynamic Quantities and Heat Capacity	140
5.2.2	Heat Capacity of Solids	141
5.2.3	Calorimetric Techniques	143
5.2.4	Background Heat Capacity	147
5.2.5	Analysis of Entropy	150
5.2.6	Magnetic Heat Capacity	153
5.2.7	Glass Transition	156
	References	158

Chapter 6 Single Crystal X-ray Structure Analysis	160
<i>Tomoji Ozeki</i>	
6.1 Introduction	160
6.2 Crystal Symmetry	161
6.2.1 Definition of Crystals	161
6.2.2 Crystal Lattice	162
6.2.3 Symmetry, Symmetry Operations, and Symmetry Elements	165
6.2.4 Category of Symmetry Operations	166
6.2.5 Crystallographic Symmetry Operations	168
6.2.6 Crystallographic Point Groups	173
6.2.7 Space Groups	175
6.2.8 Category of Space Groups: Point Groups, Laue Symmetry, and Crystal System	177
6.2.9 Point Groups and Space Groups without Inversion Centres	178
6.2.10 Bravais Lattice	181
6.3 Space Group Symbols	182
6.3.1 Triclinic Space Groups	182
6.3.2 Monoclinic Space Groups	183
6.3.3 Orthorhombic Space Groups	185
6.3.4 Tetragonal Space Groups	186
6.3.5 Trigonal Space Groups	189
6.3.6 Hexagonal Space Groups	191
6.3.7 Cubic Space Groups	192
6.3.8 International Tables	193
6.4 X-ray Diffraction by Crystals	195
6.4.1 Atomic Scattering Factors	196
6.4.2 What Determines the Diffraction Patterns?	197
6.4.3 Bragg Condition, Face Index, and Reflection Index	199
6.4.4 Laue Symmetry of Diffraction Patterns and Friedel's Law	200
6.4.5 Anomalous Scattering, Determination of Absolute Structure, and Flack Parameters	200
6.5 Diffraction Data Collection	201
6.5.1 Wavelengths	201
6.5.2 Measuring Temperatures	202
6.5.3 Crystal Selection with Visual Inspections	202
6.5.4 Mounting and Centring Crystals	203
6.5.5 Checking the Diffraction Patterns	203

6.5.6	Determination of Lattice Constants	205
6.5.7	Deciding Measurement Conditions and Starting Measurements	206
6.5.8	Integration and Correction of Raw Data	206
6.5.9	Space Group Determinations	207
6.6	Determination and Refinements of Structural Models	208
6.6.1	Initial Phase Determinations	209
6.6.2	Interpretations of the Direct Method Outputs	209
6.6.3	Disorder	210
6.6.4	Least Squares	213
6.6.5	Judgement of Convergence	214
6.7	Interpretation and Assessment of Results	214
6.7.1	Molecular Structures	214
6.7.2	Assessment of the Analysis Precision	215
6.7.3	Plausibility of the Determined Absolute Structure	216
6.7.4	Atomic Displacement Parameters	216
6.7.5	Comparison with a Database	217
6.7.6	CIF	218
6.8	Concluding Remarks	218
	References	219

Chapter 7 IR and Raman Spectroscopies 221

Junji Teraoka

7.1	Introduction	221
7.2	Interaction Between Light and Molecules	222
7.3	Molecular Vibration	226
7.3.1	Molecular Vibration of a Diatomic Molecule	226
7.3.2	Molecular Vibration of a Tri-atomic Molecule (CO_2)	227
7.3.3	Quantum Theory for Molecular Vibration	230
7.4	Molecular Symmetry	231
7.4.1	Point Groups C_{2v} and C_{3v}	232
7.4.2	Point Group $D_{\infty h}$	235
7.4.3	Selection Rules for IR and Raman Spectra	236
7.5	Resonance Raman Spectra	238
7.5.1	Selective Intensity Enhancement of the Resonance Raman Band	239

7.5.2	Which Vibrational Modes of the Chromophore Are Subject to Resonance Enhancement?	240
7.5.3	Porphyrin Ligand	241
7.6	Research Studies	242
7.6.1	Isotope Shift	242
7.6.2	Anharmonicity and Fermi Resonance	245
7.6.3	Saturation Raman Spectroscopy	245
7.6.4	Back Donation	247
7.6.5	Vibrational Circular Dichroism (VCD)	248
	Acknowledgements	249
	References	249
	Subject Index	251

Instrumental Analysis of Coordination Compounds – Volume 2

Chapter 1	Magnetic Measurement	1
<i>Masaaki Ohba and Masaki Mito</i>		
1.1	Introduction	1
1.2	Static Magnetic Measurement (DC Measurement)	2
1.2.1	Mechanical Method	4
1.2.2	Electromagnetic Induction Method	7
1.2.3	SQUID Method	10
1.2.4	Difference Between the SQUID and Electromagnetic Induction Methods – Superconducting and Normal-conducting Magnetic Flux Conversion Method	12
1.2.5	Utilization of Commercial Equipment: Magnetic Property Measurement System (MPMS) by Quantum Design (QD)	14
1.3	Magnetic Properties of Metal Complexes	18
1.3.1	Magnetic Interaction	20
1.3.2	Magnetization Curve	29
1.3.3	Ordered Magnetism	30
1.3.4	Magnetic Phase Transition Temperature T_C	33
1.4	AC Magnetic Measurement	35
1.4.1	Definition of AC Magnetic Susceptibility	35
1.4.2	Complex Magnetic Susceptibility and Linear Responsivity	36

1.4.3	Magnetic Relaxation Phenomena and Complex Magnetic Susceptibility	38
1.4.4	Measurement Method Using Hartshorn Type Bridge – Orthodox AC Measurement Method	42
1.4.5	Use of Commercial Equipment	45
1.4.6	Particular Magnetic Measurement	48
	Abbreviations	54
	References	54
Chapter 2	ESR Spectroscopy	57
<i>Takayoshi Kuroda-Sowa and Motohiro Nakano</i>		
2.1	Introduction	57
2.2	Principle of ESR	57
2.2.1	Zeeman Effect and Selection Rules	57
2.2.2	ESR of Hydrogen Atoms	58
2.2.3	Allowed Transitions and Forbidden Transitions	60
2.3	Instrument Configuration and Sample Preparation	61
2.3.1	ESR Spectrometer	61
2.3.2	Solution Sample	62
2.3.3	Solid Sample	62
2.3.4	ESR Measurements of Radicals	63
2.3.5	Detection Sensitivity	63
2.3.6	Evaluation of Spectral Parameters	63
2.4	Analyses of ESR Spectrum	65
2.4.1	Spin Hamiltonian	65
2.4.2	Tensors	66
2.4.3	Hyperfine Interaction Tensor	68
2.4.4	D-tensor (Fine Splitting Tensor)	70
2.4.5	Effect of Spin–Orbit Interaction on the Hyperfine Coupling Constant	71
2.4.6	Evaluation of Unpaired Electron Density	72
2.5	Examples of Analysis	74
2.5.1	Vanadium Complex	74
2.5.2	Copper Complex	75
2.5.3	Rhodium Dinuclear Complexes $[\text{Rh}_2(\text{O}_2\text{CMe})_4\text{L}_2]^+$	76
2.6	High Magnetic Fields EPR	77
2.6.1	Examples of HF-EPR Spectra	78
	References	86

Chapter 3 Solid State NMR Spectroscopy	89
<i>Sadamu Takeda, Hiroki Oshio and Hideki Masuda</i>	
3.1 Introduction	89
3.1.1 Magnetic Dipole Interactions Between Nuclear Spins	90
3.1.2 Anisotropy of Chemical Shifts	90
3.1.3 Solid-state High-resolution NMR (CP MAS-NMR)	90
3.1.4 Nuclear Quadrupole Interaction	90
3.1.5 Interactions Between Electron Spin and Nuclear Spin	91
3.2 Nuclear Spin in Magnetic Fields: Quantum and Classical Views	91
3.3 Manipulation of the Magnetic Moment and Nuclear Magnetization by High Frequency Pulses and NMR Signals	95
3.4 Detection of Nuclear Magnetic Dipole Interactions, Inter-nuclear Distance, and Molecular Motion in Solids	101
3.5 Magic Angle Spinning	106
3.6 High Power Decoupling	110
3.7 Chemical Shift and Its Anisotropy	111
3.8 Cross-polarization and CP MAS-NMR	116
3.9 Analysis of Molecular Motion by Nuclear Quadrupole Interaction and Deuterium NMR	122
3.10 Solid-state High-resolution NMR of Magnetic Solids: Nuclear Spin–Electron Spin Interaction	134
References	145
Chapter 4 Mössbauer Spectroscopy	147
<i>Shinya Hayammi and Hiroki Oshio</i>	
4.1 Introduction	147
4.2 Principle	148
4.3 Conditions for Mössbauer Spectroscopy	149
4.4 Practical Measurements of Mössbauer Spectra	151
4.4.1 Measuring Apparatus	151
4.4.2 Sample Preparation	152
4.4.3 Temperature Variation of the Mössbauer Spectrum	153
4.4.4 Methods for Analyzing Mössbauer Spectra	154

4.5	Mössbauer Parameters	155
4.5.1	Isomer Shift	155
4.5.2	Quadrupole Interaction	160
4.5.3	Magnetic Interaction	163
4.5.4	Time- and Temperature-dependent Effects	164
4.6	Some Problems	167
4.7	Conversion Electron Mössbauer Spectroscopy (CEMS)	169
4.8	Applications to Structural Study	171
4.8.1	$I_2Br_2Cl_4$	171
4.8.2	Xenon Chloride and Bromide	172
4.8.3	Iron Atoms and Compounds in a Matrix	173
4.9	Mössbauer Spectra of Metal Complexes with Dynamic Electronic States	174
4.9.1	Spin-crossover Iron Complexes	175
4.9.2	Photo-induced Spin Transition in Iron(II) Complexes	176
4.9.3	Mixed Valence Iron Complexes	178
4.9.4	Mössbauer Spectra Under Magnetic Fields	178
4.9.5	Synchrotron Mössbauer Spectra	178
	References	181
Chapter 5	X-ray Absorption Spectroscopy	184
	<i>Akihiro Kikuchi and Hitoshi Abe</i>	
5.1	Introduction	184
5.2	Principles of XAS Spectra	185
5.2.1	Principle	185
5.2.2	XAS Measurement of Metal Complexes	186
5.2.3	Use of Synchrotron Radiation Facilities	187
5.2.4	XANES	187
5.2.5	EXAFS	188
5.2.6	Advantages and Disadvantages of EXAFS	190
5.3	Measurement of XAS Spectra	192
5.3.1	Transmission Mode	192
5.3.2	Modes Other Than the Transmission Mode	193
5.4	Analysis of XAS Spectra	196
5.4.1	Data Preparation	196
5.4.2	XANES Analysis	198
5.4.3	EXAFS Analysis	201
5.5	Applications and Prospects of XAS	205
5.5.1	State-selective XAS	206
5.5.2	Microscopic XAS	206

5.5.3	Time-resolved XAS	207
5.5.4	Data Format and XAS Database	208
	References	208
Chapter 6	Surface Analyses Using AFM and STM	210
	<i>Soichiro Yoshimoto</i>	
6.1	Introduction	210
6.2	Principles of STM and AFM	211
6.3	Preparation for Measurements	216
6.3.1	Sample Preparation	216
6.3.2	Probe Fabrication	217
6.3.3	Preparation of Electrochemical STM Cells and Solutions	219
6.4	Calibration of the Scanner	219
6.5	Examples	220
6.5.1	Observation in Sulfuric Acid	220
6.5.2	Observation of a Pc Adlayer	222
6.5.3	Control of a Binary Array of Por and Pc	223
6.5.4	Catalytic Surface	224
6.5.5	Bi-layered Adlayer	225
6.6	Conclusions	227
	References	227
Chapter 7	Transmission Electron Microscopy	229
	<i>Hiroki Kurata</i>	
7.1	Introduction	229
7.2	Overview of a Transmission Electron Microscope	230
7.3	Electron Diffraction	233
7.3.1	Elastic Scattering of Electrons by a Single Atom	233
7.3.2	Electron Diffraction by a One-dimensional Atomic Array	234
7.3.3	Electron Diffraction by Crystals	236
7.3.4	Electron Diffraction Geometry	237
7.3.5	Nano-beam Electron Diffraction (NBED)	239
7.4	TEM Imaging and Contrast	240
7.4.1	Diffraction Contrast	241
7.4.2	Lattice Images	242
7.4.3	Lens Transfer Function	244
7.4.4	Crystal Structure Image	245
7.4.5	Practical Observation of High-resolution Images	249

<i>Contents</i>	xvii
7.5 Scanning Transmission Electron Microscopy	252
7.5.1 Imaging Principle of STEM	252
7.5.2 Principles and Features of HAADF Imaging	254
7.6 Conclusions	257
References	257
Chapter 8 Fluorescence and Phosphorescence Spectroscopy	259
<i>Masafumi Minoshima, Shahi Imam Reja and Kazuya Kikuchi</i>	
8.1 Fluorescence and Phosphorescence	259
8.2 Deactivation Process of Excited States	260
8.3 Stern–Volmer Equation	261
8.4 Examples of Relaxation Processes of Metal Complexes After Irradiation with Excitation Light and Information Obtained from Spectra	261
8.5 Fluorescence Spectrophotometer and Information Obtained	262
8.5.1 Light Source	262
8.5.2 Spectrophotometer	263
8.5.3 Sample Chamber	263
8.5.4 Detector	263
8.6 Development of Bioimaging	263
8.7 Development of Ca^{2+} Fluorescent Probes	266
8.8 Development of the Ratio Fluorescence Measurement System	268
8.9 Principle of Changing the Fluorescence Wavelength FRET	271
8.10 FRET Probe for Ca^{2+} Imaging Using GFP (Cameleon)	273
8.11 Zn^{2+} Fluorescent Probe	275
References	277
Chapter 9 Mass Spectrometry	279
<i>Kentaro Yamaguchi</i>	
9.1 Introduction	279
9.2 Overview of Mass Spectrometry	279
9.2.1 Ionization	279
9.2.2 Ion Analysis Methods	281
9.2.3 MS Spectrum Analysis	284
9.3 Mass Spectrometry of Metal Complexes	286
9.3.1 Equipment	286

9.3.2 Measurement	287
9.3.3 Analysis	288
9.4 Practical Applications of Mass Spectrometry to Metal Complexes	291
9.4.1 Tandem MS of Rare Earth Complexes	292
9.4.2 Encapsulated Complexes	294
9.4.3 Supramolecular Polymers	297
9.5 Conclusion	299
References	299
Chapter 10 Photoelectron Spectroscopy	301
<i>Toshihiko Yokoyama</i>	
10.1 Introduction	301
10.2 Principles of Photoelectron Spectroscopy	303
10.2.1 Three-step Model	303
10.2.2 Electronic Excitation Process by Photoabsorption	304
10.2.3 Inelastic Scattering and Electron Escape Depth	305
10.2.4 Electron Emission Into Vacuum and Conservation of Momentum	307
10.2.5 Kinetic Energy at the Detector	308
10.2.6 View of Measured Data and Auger Electrons	309
10.2.7 Spin–Orbit Interaction Splitting	311
10.2.8 Chemical Shift	312
10.2.9 Satellites	315
10.3 Methods of Photoelectron Spectroscopy	317
10.3.1 Introduction	317
10.3.2 Light Source	318
10.3.3 Photoelectron Energy Analyzers	321
10.4 Applications of Photoelectron Spectroscopy	323
10.4.1 Valence Phase Transitions	323
10.4.2 One-dimensional Chain Metal Complexes	325
10.4.3 Metal Phthalocyanine Thin Films	329
References	330
Subject Index	333

CHAPTER 1

Magnetic Measurement

MASAAKI OHBA^{*a} AND MASAKI MITO^b

^a Kyushu University, 819-0395 Fukuoka, Japan; ^b Kyushu Institute of Technology, 804-8550 Kitakyushu, Japan

*Email: ohba@chem.kyushu-univ.jp

1.1 Introduction

Magnetic measurements are now much more familiar to researchers in inorganic and coordination compounds than thermal and electrical resistance measurements. Electrical resistance measurements provide information on the electrical state by the contact method. Whereas magnetic measurements are performed by the non-contact method, they are convenient for evaluating the physical properties of as-synthesized samples. Magnetic measurements give information on the microscopic state of compounds, such as electronic state, structure, and magnetic interactions, as well as the macroscopic state, such as magnetic transition temperature, coercive force, magnetic domain structure, *etc.* Magnetic measurements have also become indispensable in the research fields of nano-sized magnetic materials and superconductors. Recently, magnetic measurements have become more accessible without high operating skills. Commercially available instruments are simultaneously user-friendly and highly sophisticated. However, users can fall into a trap and believe the quantified results without any doubt. It is important to always verify the data accuracy, and sometimes one needs to go back to the calculation process of the obtained data. In this chapter, we introduce basic knowledge of the measurement devices and methods and show some examples of analyzing the magnetic properties of coordination compounds.

Most chemists nowadays use electromagnetic induction style devices or superconducting quantum interference devices (SQUIDs) for magnetic

measurements. In this chapter, we focus on these measurement methods, divided into **static magnetic measurement (DC measurement)** to detect the magnitude of the magnetic momentum and **alternating current magnetic measurement (AC measurement)** to detect the dynamic magnetic response to periodic external fields. In particular, the AC measurement, being indispensable for evaluating magnetic properties, is introduced in detail.

The DC measurement provides the fundamental magnetic properties of compounds (paramagnetism, diamagnetism, magnetic interactions, *etc.*) as the temperature- and field-dependences of the magnetic susceptibility. It has been easier for chemists to carry out measurements at high cryogenic temperatures and high magnetic fields with the cooperation of physicists so far. In recent years, chemists have been able to work at cryogenic temperatures of 0.5 K and with high magnetic fields of 10 T (tesla) in their laboratories, although it is still difficult to use pulsed high magnetic fields. On the other hand, the AC measurement is an important method to evaluate the dynamic magnetization process, which yield essential data for the magnetic property analysis of single molecule magnets, single ion magnets, single chain magnets, spin qubits, *etc.* The AC measurements are divided into the 10^{-2} Hz to 1 kHz range using SQUID and the 10 Hz to 10 kHz range using electromagnetic induction-based devices. The AC magnetic susceptibility data over a wide frequency range have become essential in recent research on nano-sized magnetic materials for magnetic recording media and medical applications. Here, it should be noted that commercially available magnetic measurement devices automatically correct for eddy current effects and calculate the complex magnetic susceptibility, due to the presence of metallic materials in the space where the AC magnetic field is applied. It is essential to understand this point when attempting high-pressure experiments using a pressure cell partly made of metal. The various magnetic measurement methods presented in this chapter are classified into three levels, and their characteristics are compared in Table 1.1.^{1,2} The details are explained below.

1.2 Static Magnetic Measurement (DC Measurement)

When a substance with magnetic moment \mathbf{m} is placed in a magnetic field, the substance creates a new magnetic field called magnetization. The magnetization value (\mathbf{M}) in response to the uniform and steady (no time variation) static magnetic field (\mathbf{H}) is called a magnetization curve. Usually, when the magnetic field \mathbf{H} is increased from zero, the magnetization \mathbf{M} , which corresponds to the magnetic moment per unit volume, is proportional to \mathbf{H} in the small magnetic field (eqn (1.1)).

$$\mathbf{M} = \gamma \mathbf{H} \quad (1.1)$$

Table 1.1 Categorization of magnetic measurements.

Large category	Middle category	Small category	Observed physical quantity	Measurement accuracy [emu]	Feature
Static (DC) magnetic measurements	Dynamical methods	Magnetic balance	Vertical magnetic force	10^{-6}	Simple electric and mechanical system, zero field measurement is possible
		Magnetic pendulum	Horizontal magnetic force	10^{-6}	No influence of gravity
		Cantilever	Torque	$<10^{-10}$	High field measurement is possible
	Electromagnetic induction method	Capacitance method	Vertical magnetic force	10^{-6}	Suitable for low temperature measurement because of small heating
		Extraction methods	Electromotive force	10^{-5}	Suitable for high field, high pressure, and low temperature
		Sample vibration method	Electromotive force	10^{-6}	Lock-in detection is promising
	SQUID method	Coil vibration method	Electromotive force		Lock-in detection is promising
		DC magnetic method	Magnetic flux	10^{-8}	High accuracy, most conventional method
		Sample vibration method	Magnetic flux	10^{-8}	Lock-in detection is promising
		Coil vibration method	Magnetic flux	$<10^{-9}$	Lock-in detection is promising
Alternating current (AC) magnetic measurements	Electromagnetic induction method		Electromotive force	10^{-7}	Promising for high frequency measurements
	SQUID method	Superconducting magnetic flux transformation	Magnetic flux	10^{-8}	Promising for low frequency measurements

The slope χ evaluated within the linear relationship of the \mathbf{M} and \mathbf{H} values is called the susceptibility or magnetic susceptibility. χ is usually calculated by dividing \mathbf{M} by \mathbf{H} in the DC measurements. Here, \mathbf{M} includes the contribution from the diamagnetic field due to diamagnetic components. If only the magnetically active elements are to be evaluated using eqn (1.1), a correction for the diamagnetic field is necessary.³ There are various methods for measuring \mathbf{M} , unlike AC susceptibility (see Section 1.4); **static magnetic measurements** detect the magnitude of \mathbf{M} in a static magnetic field that does not change over time.

Next, the units of the magnetic field should be mentioned. The relationship between the magnetic flux density \mathbf{B} and the magnetic field \mathbf{H} is as follows.

$$\mathbf{B} = \mu_0 \mathbf{H} \quad (1.2)$$

Table 1.2 lists units of \mathbf{H} and \mathbf{B} . In the cgs unit system, the unit of \mathbf{H} is Oe (oersted) and \mathbf{B} is G (gauss). By convention, G is often used as the unit for \mathbf{H} in the sense of the value of \mathbf{H} corresponding to \mathbf{B} , based on the assumption that $1 \text{ Oe} = 1 \text{ G}$ from the vacuum permeability $\mu_0 = 1$. In this case, emu (electromagnetic unit) is used as the unit of magnetic susceptibility χ .

In this chapter, the static magnetic measurements (DC methods) are classified into three methods; the mechanical method, which measures the force acting on substances (Section 1.2.1), the electromagnetic induction method, which measures induced electromotive force using electromagnetic induction (Section 1.2.2), and the superconducting quantum interference device (SQUID) method (Section 1.2.3). Some consider the SQUID method, which uses mutual induction in the magnetic flux conversion between the pick-up coil system and the SQUID, to be included in the electromagnetic induction method. But since its characteristics differ from the original electromagnetic induction method, this chapter describes the SQUID method separately from the electromagnetic induction method.

1.2.1 Mechanical Method

The mechanical method has been used before the SQUID method became popular. This method measures the magnetic force exerted on a magnetized sample by the non-uniform magnetic field between

Table 1.2 Magnetic field and magnetic flux density units.

	Symbol	cgs unit system	Conversion constant (cgs→SI)	SI unit system
Magnetic field	H	Oe	$10^3/4\pi$	A m^{-1}
Magnetic flux density	B	G	10^{-4}	T

the poles of an electromagnet. When a substance with magnetic moment \mathbf{m} is placed in a magnetic field \mathbf{H} , the magnetic energy is $-\mathbf{m} \cdot \mathbf{H}$. The following equation expresses the force \mathbf{F} acting on the magnetic moment.²

$$\mathbf{F} = -\text{grad}(-\mathbf{m} \cdot \mathbf{H}) \quad (1.3)$$

$$= \mathbf{m} \times \text{rot} \mathbf{H} + \mathbf{H} \times \text{rot} \mathbf{m} + (\mathbf{H} \cdot \text{grad})\mathbf{m} + (\mathbf{m} \cdot \text{grad})\mathbf{H} \quad (1.4)$$

Here, all terms on the right-hand side of eqn (1.4) are zero except for the fourth term, assuming no current ($\text{rot} \mathbf{H} = 0$) and uniformly-magnetized sample, then the following equation is obtained.

$$\mathbf{F} = (\mathbf{m} \cdot \text{grad})\mathbf{H} \quad (1.5)$$

To consider eqn (1.5) in detail, place the sample at the position where the magnetic field gradient is maximum between the poles of the electromagnet (Figure 1.1). In this case, the magnetic field is $\mathbf{H} = (H_x, 0, 0)$. If the effect of magnetic anisotropy in the crystal is ignored, the magnetic moment \mathbf{m} is directed to the magnetic field direction. That is, $\mathbf{m} = (m_x, 0, 0)$. In addition, the relationship $\partial H_x / \partial x = \partial H_y / \partial x = 0$ holds when an electromagnet with symmetrical poles is used. In this case, the force \mathbf{F} is expressed by eqn (1.6).

$$\mathbf{F} = \left(m_x \frac{\partial H_x}{\partial x}, m_x \frac{\partial H_y}{\partial x}, m_x \frac{\partial H_z}{\partial x} \right) = \left(0, 0, m_x \frac{\partial H_z}{\partial x} \right) \quad (1.6)$$

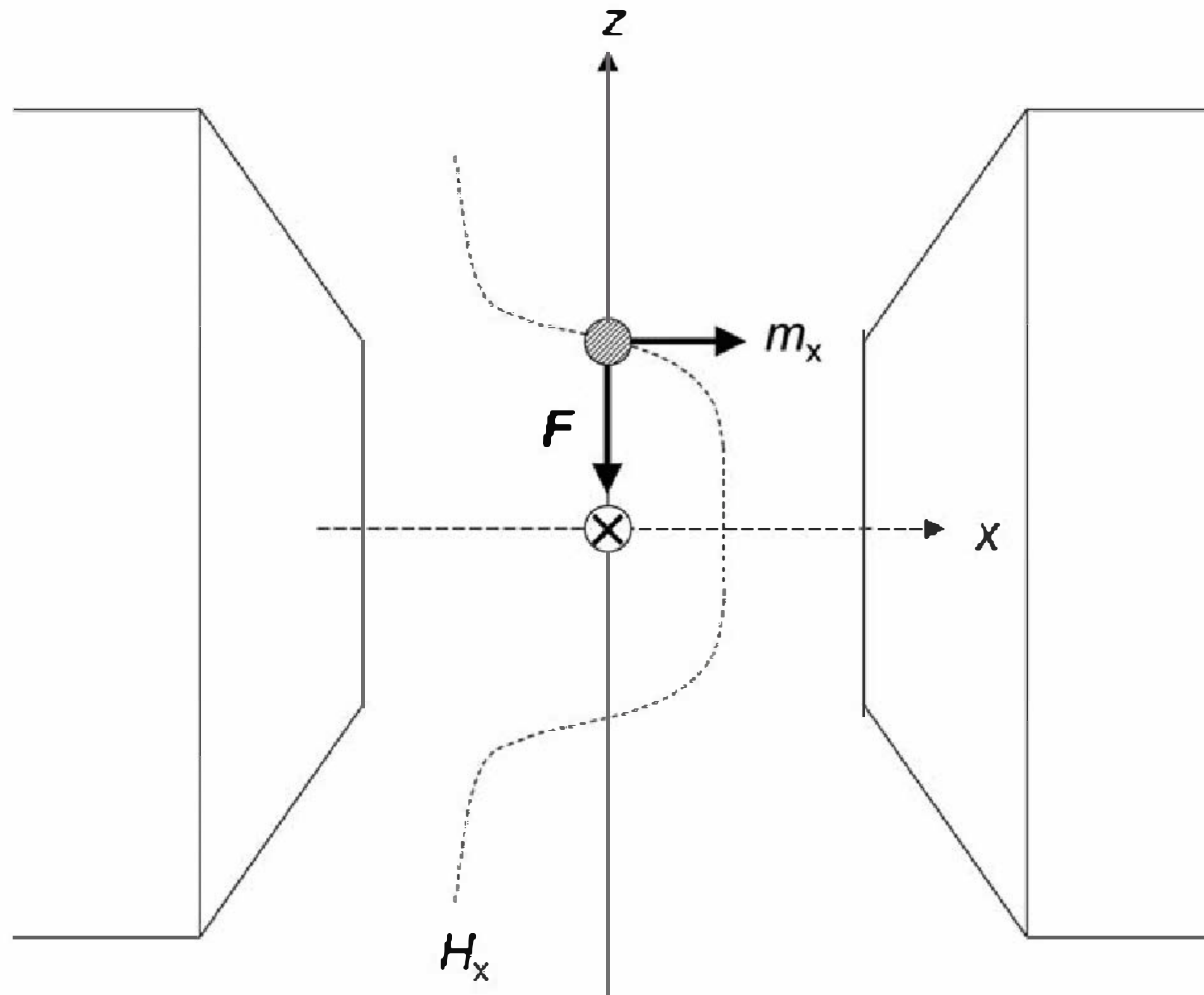


Figure 1.1 Force \mathbf{F} acting on a sample placed in a gradient magnetic field between the poles of an electromagnet.²

Here, $\partial H_z / \partial x = \partial H_x / \partial z$ from the condition $\text{rot } \mathbf{H} = 0$, which leads to eqn (1.7).

$$\mathbf{F} = \left(0, 0, m_x \frac{\partial H_x}{\partial z} \right) \quad (1.7)$$

The magnetic moment \mathbf{m} can be calculated by measuring the force \mathbf{F} acting on the sample placed in a non-uniform magnetic field. For the actual force measurement, we need to keep the sample at the position of the maximum magnetic field gradient, so the zero-detection method, which feeds back a signal proportional to the force, is used. The disadvantage is that the magnetic field of the electromagnet cannot be used effectively because the sample is not located at the position of the maximum magnetic field.

A representative apparatus for mechanical methods is the magnetic balance magnetometer (Faraday method), which uses a balance for weighing. As shown in Figure 1.2, a sample is suspended between the poles of electromagnets, and feedback coils are placed on the other side, in which a permanent magnet is suspended. When a current is applied to the feedback coil to keep the balance, the magnitude of \mathbf{F} is measured from the magnitude of the current. Since we measure forces in the direction of gravity here, we need to compensate for the contribution of additional forces except for magnetic forces.

On the other hand, pendulum-type magnetometers measure the force acting in the horizontal plane, so only the magnetic force is measured. In both cases, the magnetic moment \mathbf{m} can be evaluated by measuring the magnetic force using a balance. While magnetic balances have good sensitivity, they are not suitable for measurement in strong magnetic fields due to their instability against lateral shaking. Recently, strain gauges (commonly known as load cells) have been used for force detection. Among them, a small cantilever can be applicable for measurement under a strong magnetic field.

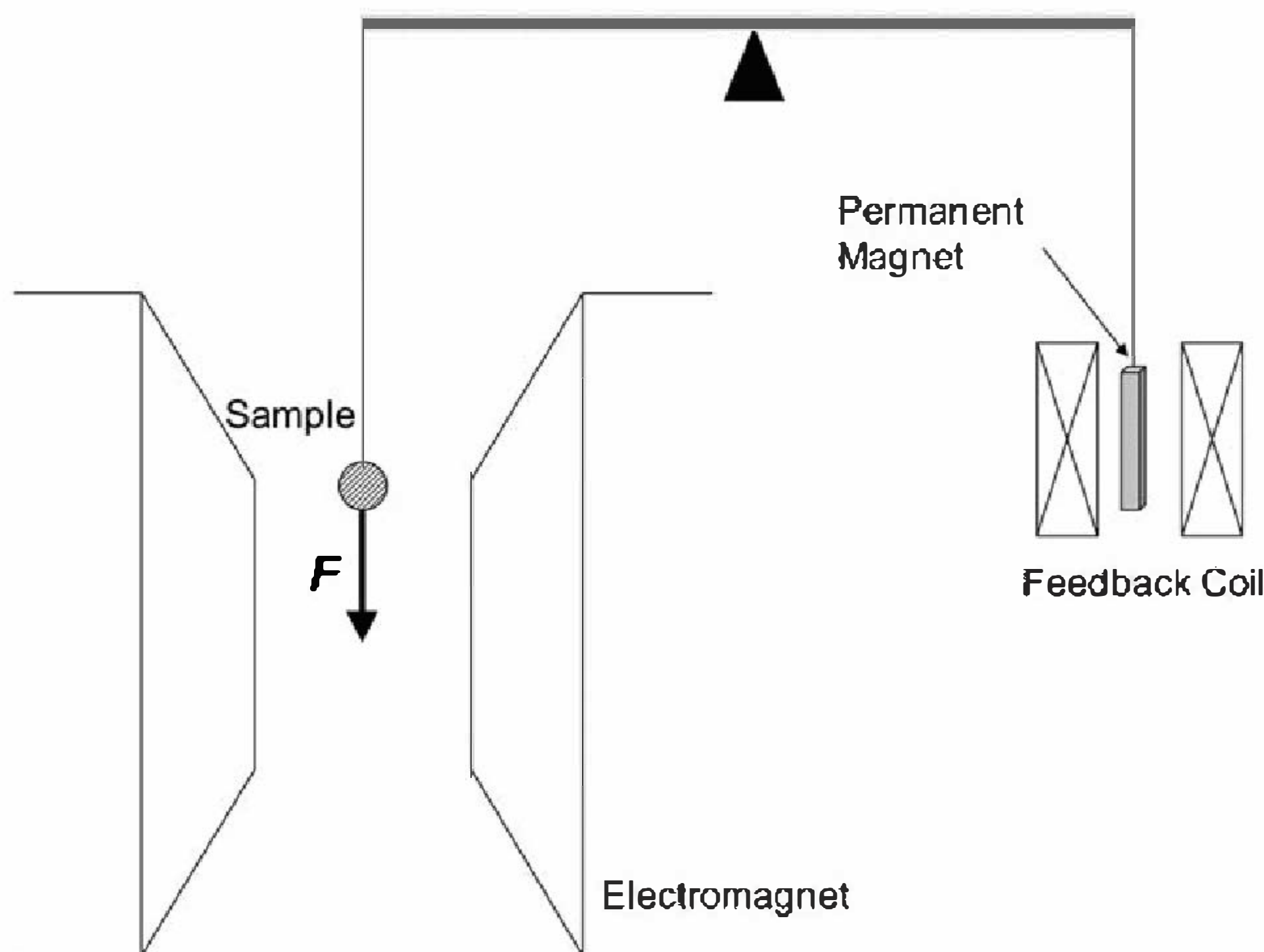


Figure 1.2 Schematic of a Faraday balance magnetometer.²

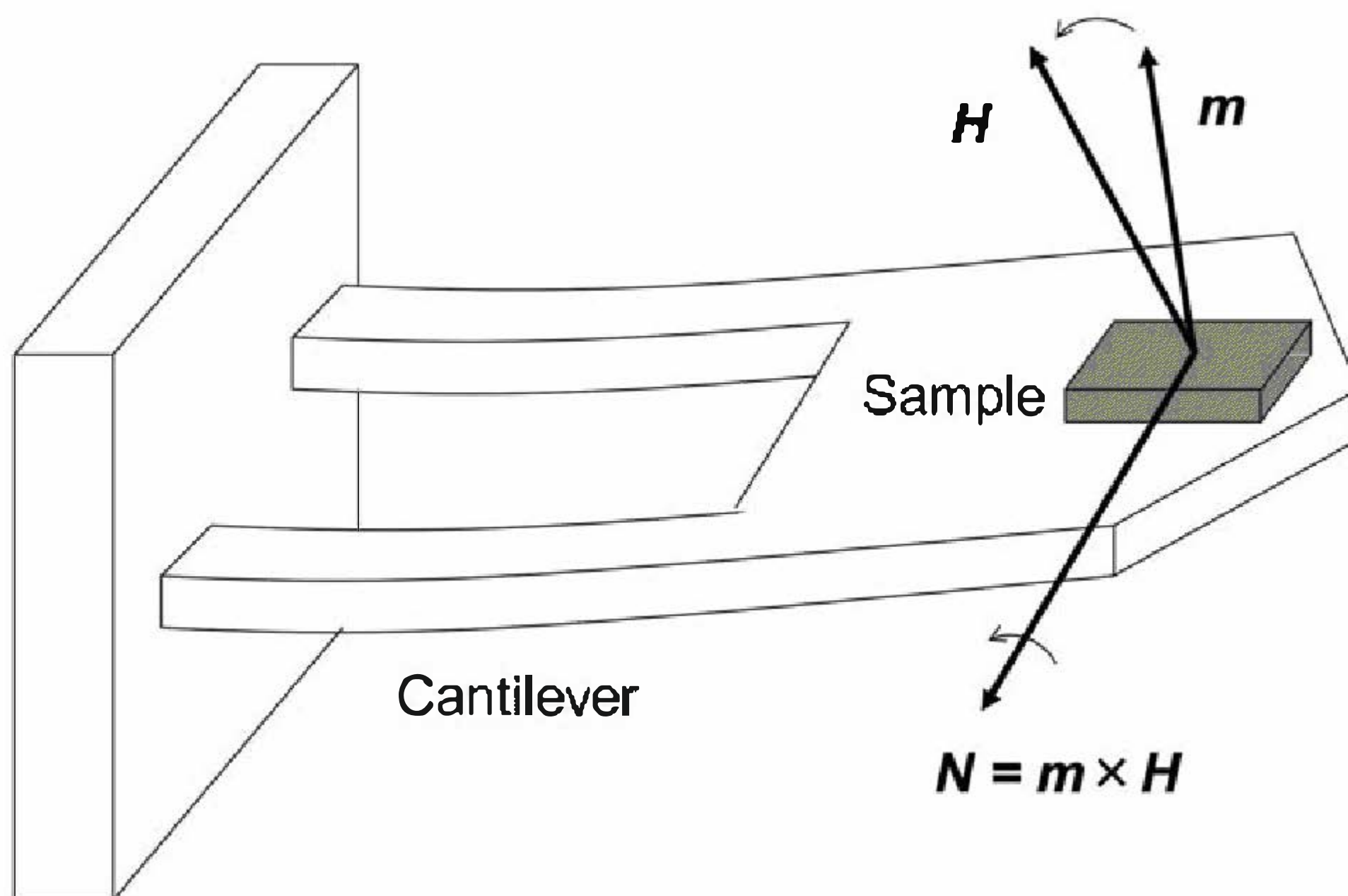


Figure 1.3 Principle of magnetic measurement using cantilevers.⁴

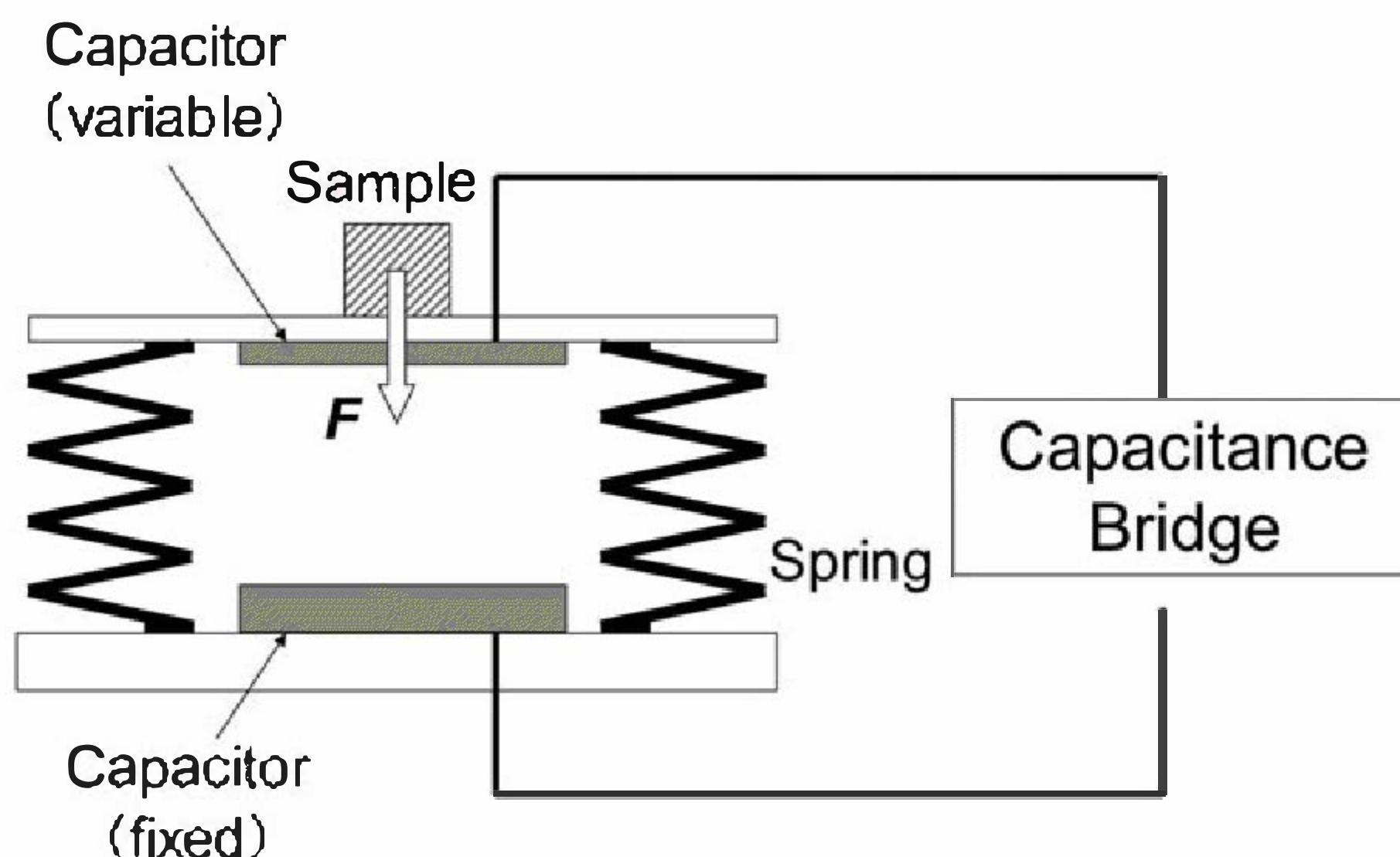


Figure 1.4 Principle of the capacitance method.⁵

Moreover, due to its high natural frequency, it is also applicable under pulsed high magnetic fields. As shown in Figure 1.3, the torque N acting between the magnetic field H and the magnetic moment m of the sample on the cantilever causes deflection of the cantilever, which is detected as a change in electrical resistance.⁴ There is also a method to measure magnetic force through changes in the capacitance of a parallel plate capacitor (capacitance method), as shown in Figure 1.4. This method is used for static magnetic measurements in cryogenic regions because there is no friction due to sample movement and no heat generation due to induced currents.⁵

1.2.2 Electromagnetic Induction Method

The electromagnetic induction method measures the induced electromotive force in the form of an induced voltage generated in the direction that interferes with the change in the magnetic flux penetrating the pick-up coil.

When the magnitude of the magnetization M of the sample in a uniform magnetic field or the relative position of the sample to the pick-up coil changes with time, the pick-up coil generates an induced electromotive force V proportional to the time derivative of the magnetic flux Φ that penetrates the pick-up coil (eqn (1.8)).

$$V = - \frac{d\Phi}{dt} \quad (1.8)$$

From the relation $\Phi = kM$ (k is the proportional constant), M is obtained as the integral value of eqn (1.8) concerning time, where k depends on the sample shape, coil shape, etc.

$$M = \frac{1}{k} \int_0^t V dt \quad (1.9)$$

There are four representative methods for generating induced electromotive force.

- (1) Vibrate the sample between the pick-up coils (**vibrating sample magnetometer (VSM) method**, Figure 1.5(a)).
- (2) Vibrate the pick-up coils around the sample (**vibrating coil magnetometer (VCM) method**, Figure 1.5(b)).
- (3) Move the sample in a certain direction in the pick-up coil (**extraction method**).
- (4) Vary the magnetic field (**pulse magnetic field measurement**, **AC magnetic susceptibility measurement**).

For (1) and (2), the induced electromotive force V shows a periodic variation concerning time, while for (3), it does not. For (4), when a pulsed magnetic field is used, V shows a non-periodic time variation, and M can be

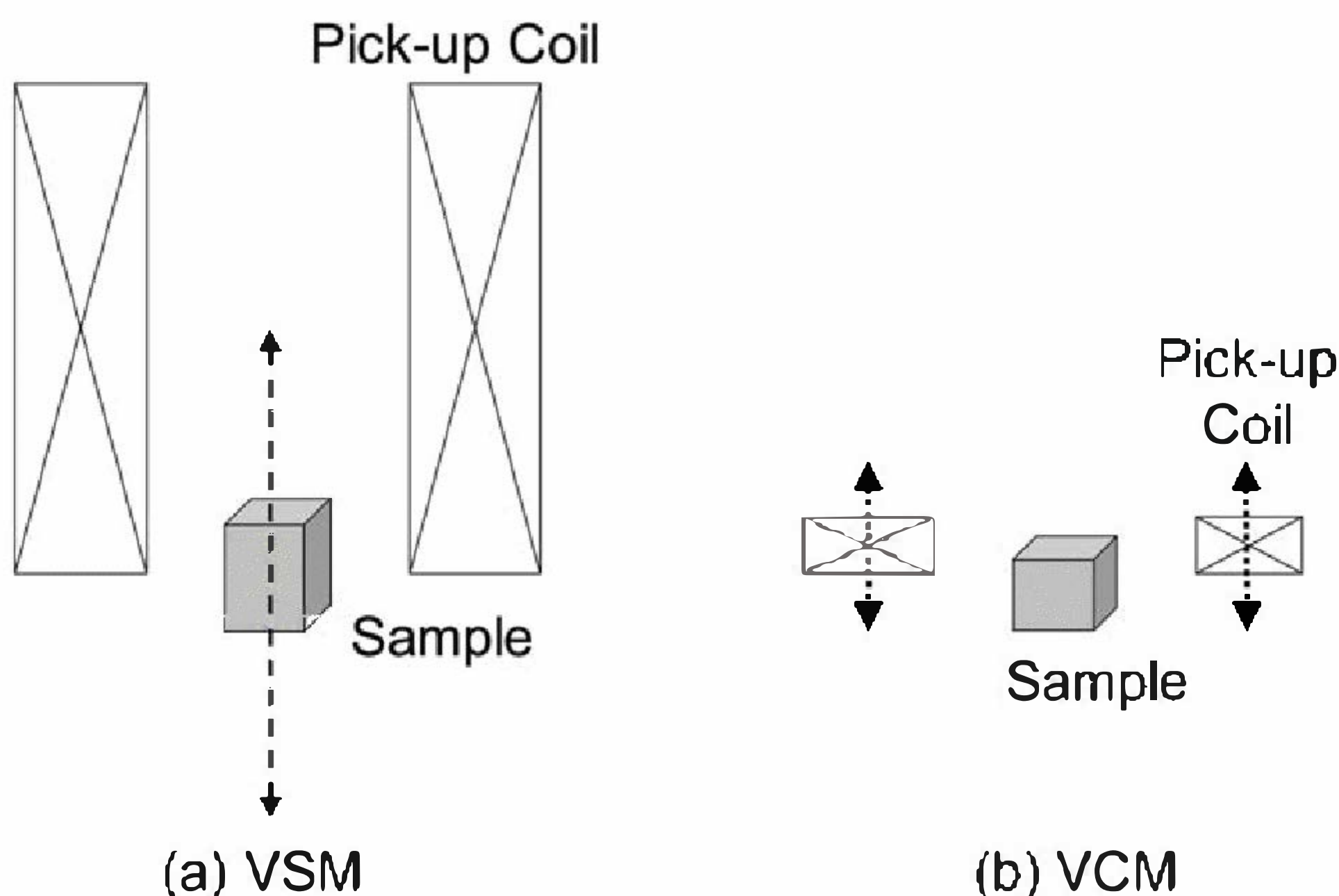


Figure 1.5 (a) VSM method and (b) VCM method.

calculated by integrating V over time (eqn (1.9)). In the case of (4) using AC magnetic field, V will show a periodic time variation and give an AC magnetic susceptibility, which is out of the category of DC measurement. Methods (1)–(3) are outlined below.

- (1) **The vibrating sample magnetometer (VSM)** uses a coil to detect changes in magnetic flux when a magnetized sample is vibrated at a constant frequency, where the generated induced electromotive force V is proportional to the magnetization value M of the sample. The vibration amplitude is calculated by lock-in detection, which has the advantage that the signal can be separated from noise components such as power supply noise. The pick-up coils may be located away from the sample but are often placed in the vicinity of the sample. Since the VSM method is a relative measurement, it must be calibrated using a standard sample with a known magnetization value to evaluate the absolute value in the measurement. With this in mind, the VSM is the most versatile magnetization measurement device using the electromagnetic induction method at the laboratory level.
- (2) **The vibrating coil magnetometer (VCM)** is an apparatus in which the sample position is fixed, and the pick-up coil is vibrated. When a thin pick-up coil is used, it is vibrated near the position where the magnetic flux from the sample changes with the largest position derivative.⁶ So, it is not always good to place the pick-up coils at the same height as the sample. VCM is effective when the sample and pick-up coils must be spatially separated, but it is less popular than VSM.
- (3) **The extraction method** has long been used in many high magnetic field facilities to measure magnetization curves under high magnetic fields. The advantage is that measurements can be performed efficiently even with slow sweep-speed magnets, such as high-field superconducting magnets. However, since the sample is moved significantly between the coils, magnetization and demagnetization are repeated at each sample movement. This has the disadvantage that the measured value fluctuates per measurement for samples exhibiting magnetic hysteresis, such as in ferromagnetic materials. Figure 1.6 shows an example of the extraction method using a superconducting magnet. This system is designed to measure under multiple extreme environments of high magnetic field, high pressure, and low temperature.⁷ Figure 1.7 shows the change in induced voltage V_1 when the sample is extracted from the pick-up coils. Point A is the starting point of the movement, and the voltage at point A is the offset voltage V_0 . Between points B and C, the sample moves inside the space between the pick-up coils. The area of the shaded part is determined from the maximum and minimum values of the induced current I . It is proportional to the M of the sample, independent of the sample extracting speed.

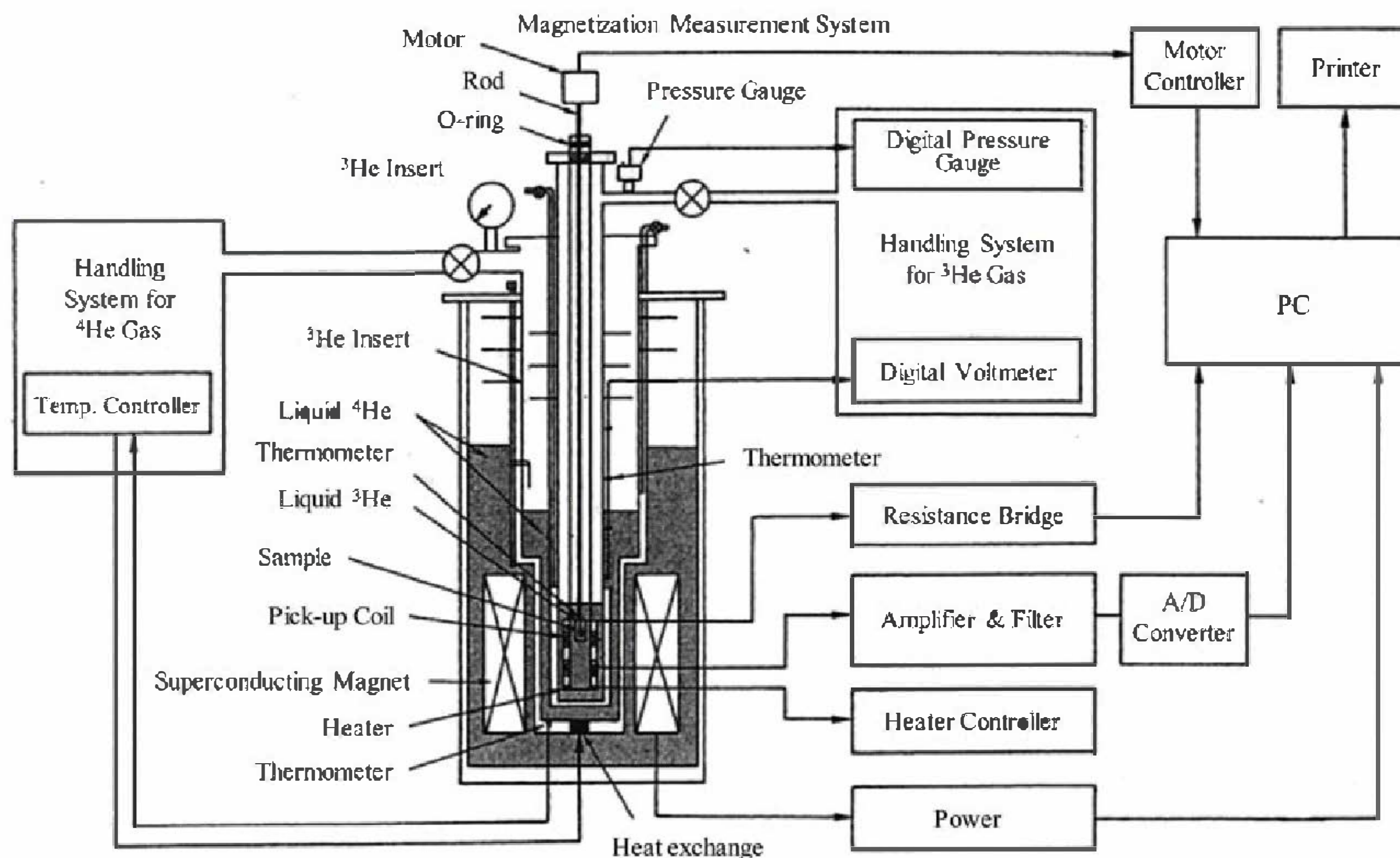


Figure 1.6 Block diagram of the magnetization measurement system using the extraction method under multiple extreme conditions of the high magnetic field, high pressure, and low temperature.⁷ Adapted from ref. 7 with permission from AIP Publishing, Copyright 1998.

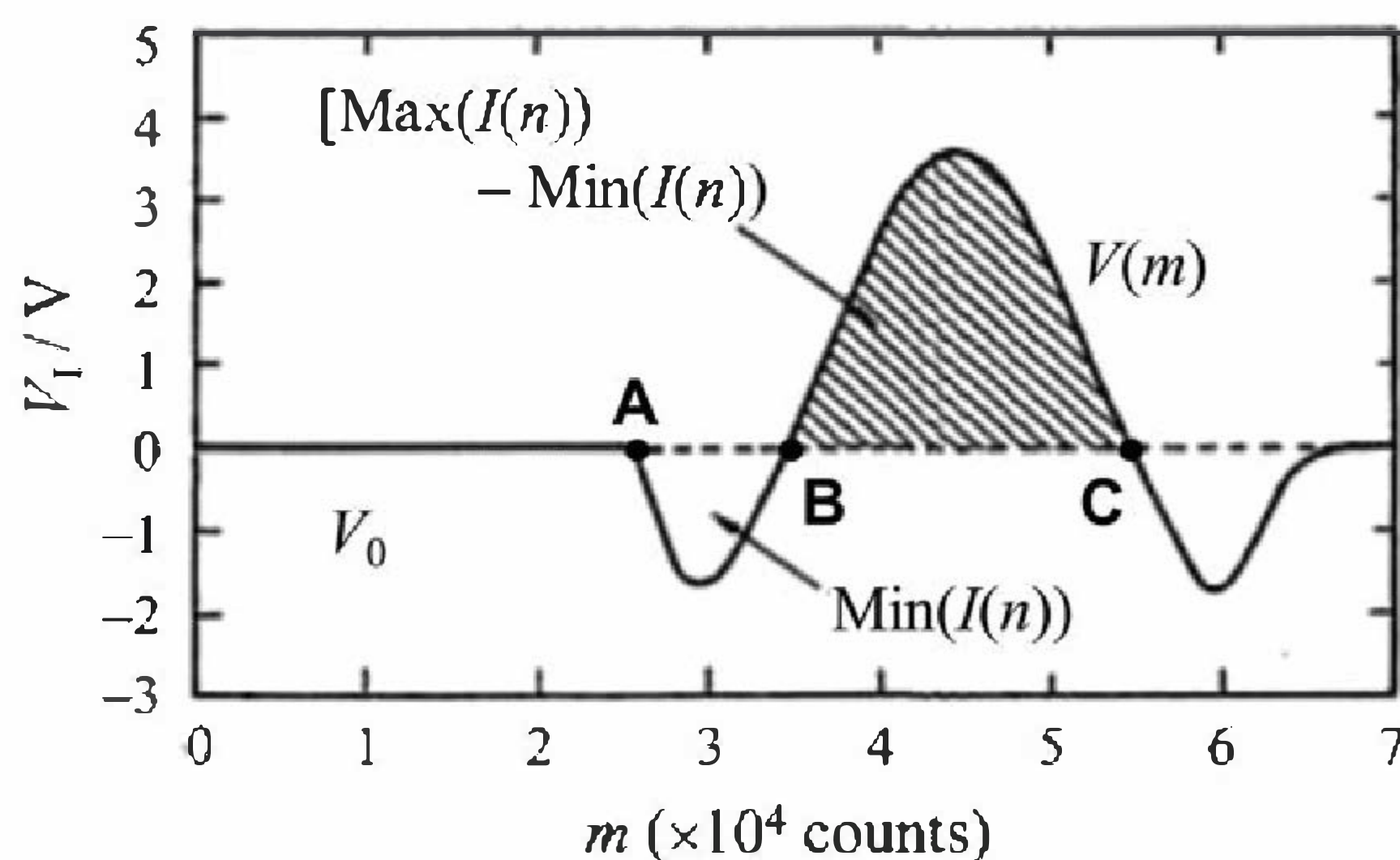


Figure 1.7 Variation of the signal voltage generated in the magnetization pick-up coils by the extraction method. The area of the shaded part is proportional to M of the sample.⁷ Adapted from ref. 7 with permission from AIP Publishing, Copyright 1998.

1.2.3 SQUID Method

A SQUID is a weakly coupled superconducting device (Josephson junction) that can directly measure changes in the magnetic flux Φ . The tunnel current flowing between junctions is modulated by the number of magnetic fluxes, and the voltage across SQUID has periodic characteristics concerning changes in magnetic flux. A SQUID magnetometer measures the number of magnetic fluxes produced by a sample as quantum flux Φ_0 ($= 2.06783461 \times 10^{-15}$ Wb)

units using the above principle. The basic structure of a SQUID magnetometer consists of a SQUID for magnetic flux detection, a magnetic flux conversion circuit that transmits the magnetic flux of the measurement space to the magnetic flux detection section, and an electronic circuit to extract voltage signals from the SQUID. Typically, a feedback mode is used to linearize the nonlinear characteristics between the voltages across the SQUID and the magnetic flux changes. Such a flux-locked loop (FLL) circuit, commonly called the zero detection method, can provide a detection sensitivity that is about 1/100 for Φ_0 . The measurement sensitivity is superior to other general-purpose measurement methods.

There are two types of SQUIDS: rf-SQUIDS, which have one Josephson junction in the superconducting ring, and dc-SQUIDS, which have two.^{8,9} Figure 1.8 shows a block diagram of the rf-SQUID system.⁸ Firstly, the tank circuit (LC parallel resonance circuit) is excited by a constant current source at its resonant frequency (typically in the rf band of 20–30 MHz). The rf-SQUID is driven by circulating current in the ring due to electromagnetic induction. The voltage of the tank circuit coupled to the rf-SQUID is amplified and detected, followed by phase detection at the modulation frequency. The output is fed back to the SQUID by a resistor R_{FB} and feedback coil. Figure 1.9 shows an example block diagram of a dc-SQUID system driven by a DC current source. While rf-SQUIDS resist external disturbances (noise), they are inferior to dc-SQUIDS in terms of sensitivity. On the other hand, dc-SQUIDS have the advantages of high sensitivity and fast response but are more susceptible to external disturbances than rf-SQUIDS.

The advantage of SQUIDS is that they can provide high reliability as well as high measurement accuracy when fabricating general-purpose devices. However, there is a problem that the pick-up coil, which consists of a superconducting wire (typically NbTi with a superconducting transition temperature of 9 K), must be maintained below the superconducting transition temperature during the measurement. To perform measurements over

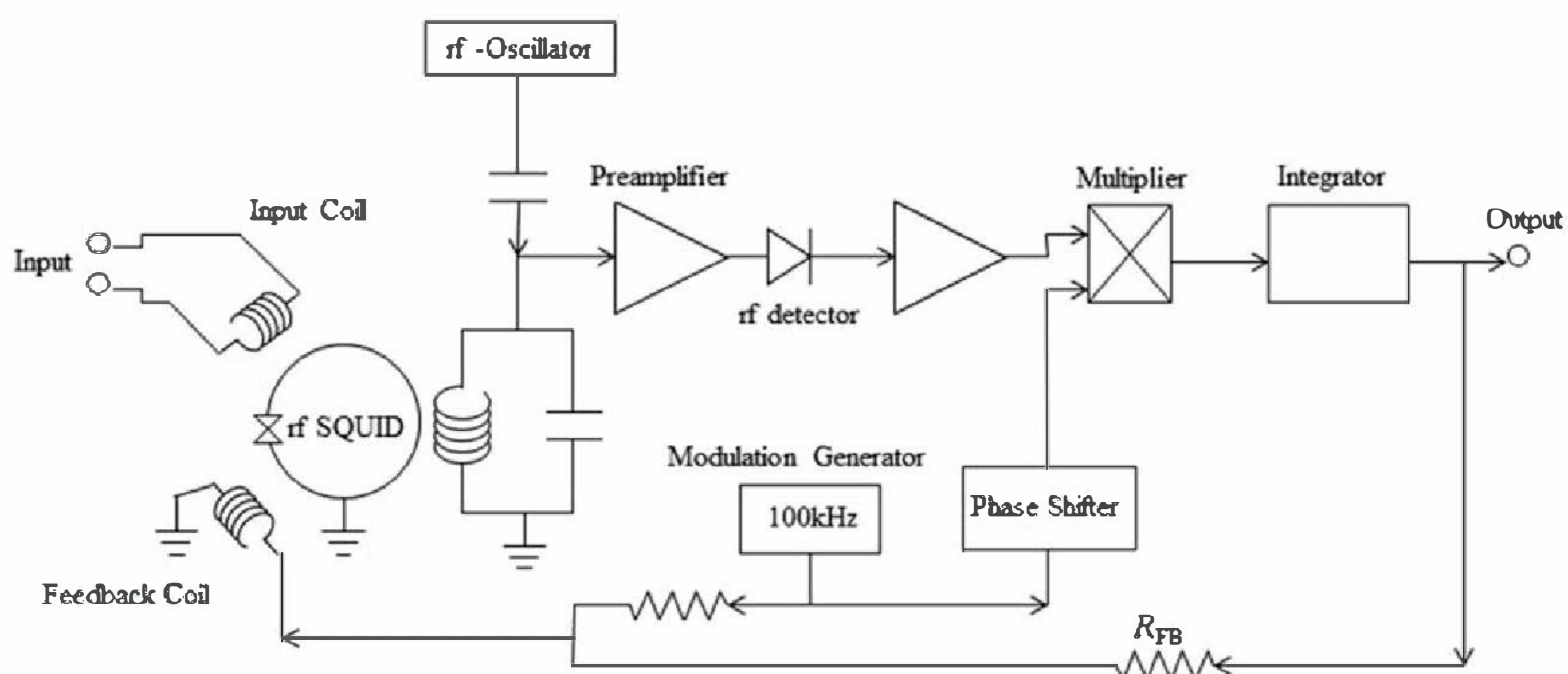


Figure 1.8 A block diagram of the rf-SQUID system.⁸

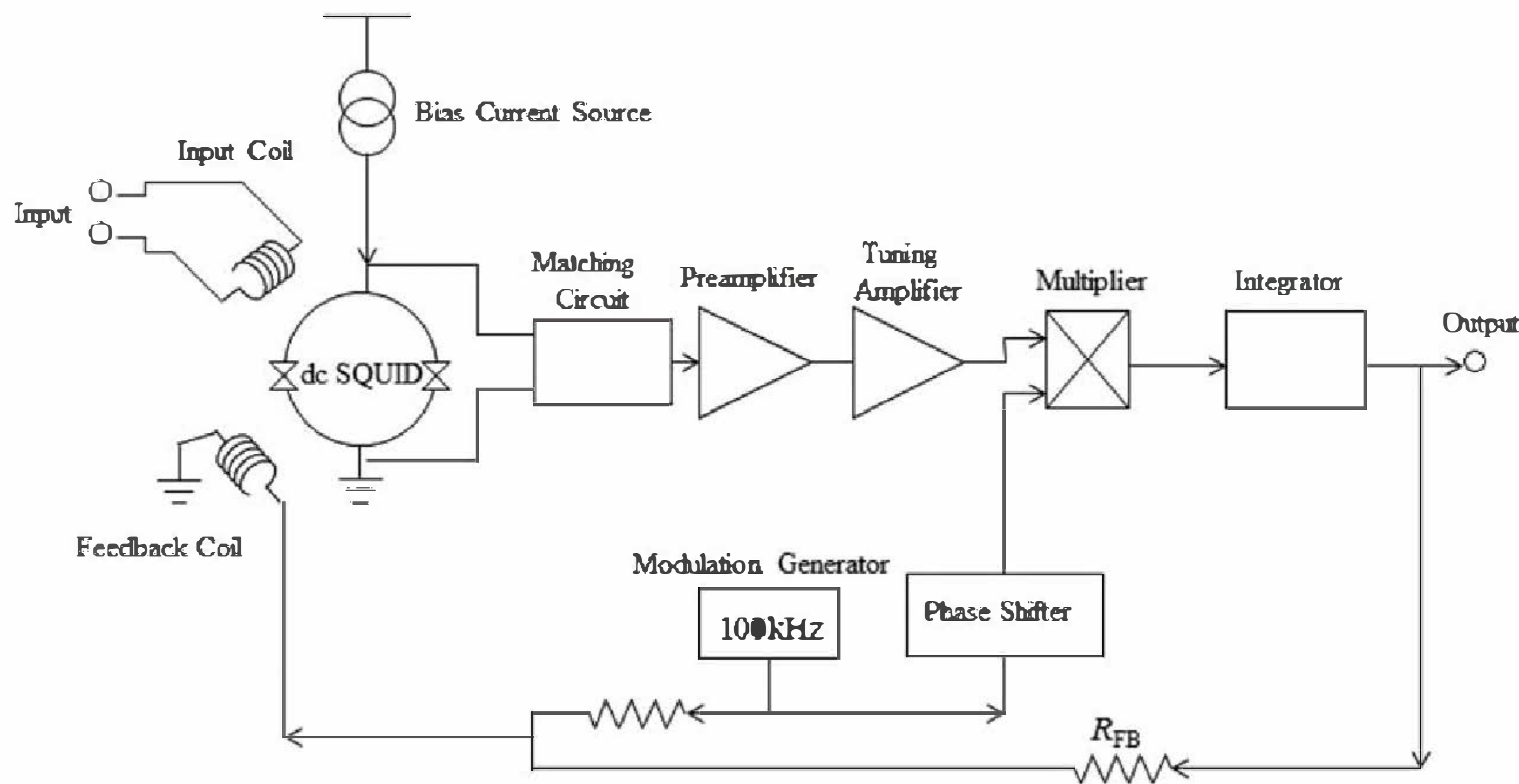


Figure 1.9 A block diagram of the dc-SQUID system.⁸

a wide temperature range, the pick-up coil must be thermally isolated from the sample space and placed in a low-temperature heat bath, even at the expense of detection sensitivity. If the pick-up coil is placed close to the sample to increase its filling factor, the temperature of the pick-up coil may increase with increasing the sample temperature, which will cause the SQUID system to fail.

1.2.4 Difference Between the SQUID and Electromagnetic Induction Methods – Superconducting and Normal-conducting Magnetic Flux Conversion Method

The SQUID method includes the micro-SQUID method, in which the SQUID itself is used as the pick-up coil, but this is not suitable for conventional SQUID magnetometers in which the sample is frequently replaced. Therefore, we place the sample at a distance from the SQUID and use a mechanism to transmit the change in magnetic flux to the SQUID. Usually, a magnetic flux conversion circuit is employed for this mechanism, in which a closed loop is formed with the pick-up coil that detects the magnetic flux of the sample, and the signal coil that transforms the magnetic flux signal to the SQUID (Figure 1.10). Here, the self-inductance of the SQUID is described as L , and the self-inductance and the winding number of both the pick-up coil and the signal coil are described L_1 , n_1 , and L_2 , n_2 , respectively. The optimization of this magnetic flux conversion circuit is so important that it affects the accuracy of magnetic measurements. Consider the following two cases; case 1, that all of the magnetic flux conversion circuits are in the superconducting state, and case 2, that some or all are in the normal conducting state. Case 2 corresponds to the abovementioned case of which the pick-up coil made of superconducting wire is placed close to the sample and

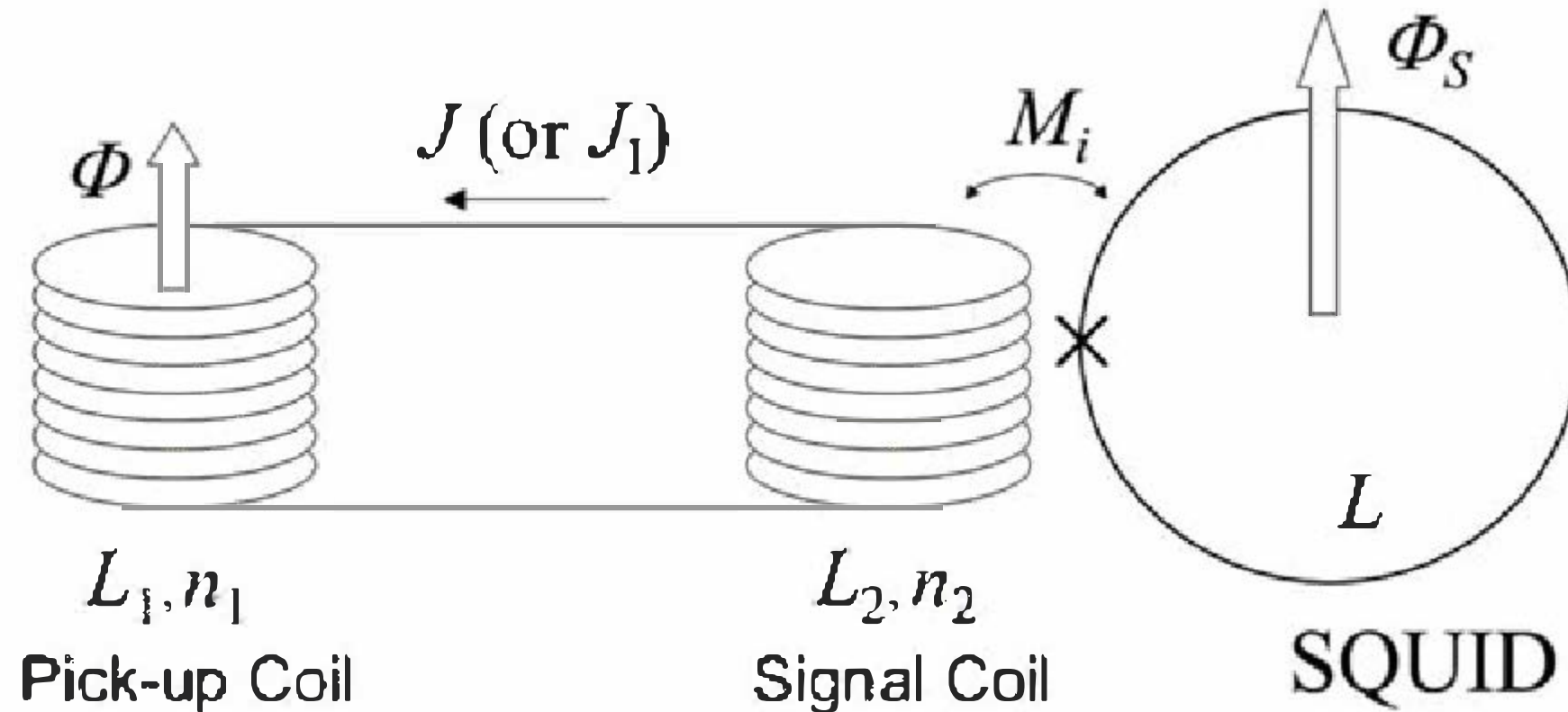


Figure 1.10 Magnetic flux conversion circuit.

changed to the normal-conductive state due to the sample temperature increase.

When the magnetic flux conversion circuit is all in a superconducting state and a superconducting closed loop is realized, it is called a superconducting magnetic flux conversion scheme. In this circuit, the magnetic flux Φ penetrating the circuit is kept constant. If the pick-up coil senses a magnetic flux change in Φ , the superconducting current I flows through the circuit, which counteracts the change, satisfying eqn (1.10).

$$\Phi n_1 + (L_1 + L_2)I = 0 \quad (1.10)$$

In this case, a magnetic flux change $\Phi' = L_2 I$ is induced in the signal coil, which is equal in magnitude but opposite in sign to that of the magnetic flux change in Φ . The magnetic flux change Φ in the signal coil provides magnetic flux Φ_S to the SQUID through mutual inductance M_i .

$$\Phi_S = M_i I \quad (1.11)$$

The advantage of this detection method is that it can transmit a direct current (steady) signal using a superconducting current always flowing in the circuit, *i.e.*, directly detecting static magnetization. Here, the relationship, eqn (1.12), is held between the magnetic flux change in Φ detected in the pick-up coil and the magnetic flux Φ_S transmitted to the SQUID.

$$\Phi_S = - \frac{M_i n_1}{L_1 + L_2} \Phi \quad (1.12)$$

The coils should be designed to maximize Φ_S so that $M_i n_1 / (L_1 + L_2)$ is maximized. Maximizing $M_i n_1 / (L_1 + L_2)$ and increasing M_i makes the coupling constant K ($K^2 = M_i^2 / L_1 L_2$) close to 1, finally leading to the condition of $L_1 = L_2$.

Next, consider the case where the superconducting loop of the magnetic flux conversion circuit is fallen to normal-conductive. This is the normal-conducting magnetic flux conversion scheme instead of the superconducting one described above. When a time-varying magnetic flux Φ is given to the pick-up coil, an induced electromotive force V is generated in the circuit and an induced current I_1 flows accordingly. V and I_1 through the circuit are given by eqn (1.13) and (1.14), respectively, where Z_1 ($= i\omega L_1$) and Z_2 are the